Acta Geochim (2022) 41(3):453–469
https://doi.org/10.1007/s11631-022-00534-1

ORIGINAL ARTICLE

Magma mixing dynamics in a vertically zoned granitic magma chamber inferred from feldspar disequilibrium assemblage and biotite composition: a case study from the Mikir Massif, eastern India

Gaurav Hazarika[1] · Pallabi Basumatary[1] · Tribujjal Prakash[1] · Hiredya Chauhan[2] · Bibhuti Gogoi[1]

Received: 16 November 2021 / Revised: 14 January 2022 / Accepted: 3 February 2022 / Published online: 6 April 2022

Abstract The Kathalguri Pluton is a granitic pluton confined within the Palaeo-Mesoproterozoic Shillong Group of rocks in the Mikir Massif, eastern India. The pluton is vertically zoned characterized by lower medium- to coarse-grained equigranular to porphyritic granite and upper fine-grained equigranular granite. Small to large mafic magmatic enclaves (MME) are distributed within the lower granite, while homogeneous grey-coloured hybrid rocks dominate the upper granite. From field relationships, textural features, and mineral chemical analyses we infer that the Kathalguri Pluton was a vertically zoned felsic magma chamber that was intruded by mafic magma during its evolution. The lower portion of the magma chamber was occupied by crystal mush, while the upper portion was dominated by melt when mafic magma intruded it. The occurrence of upper and lower zonations was probably brought about by fractional crystallization. The presence of such zonations within the felsic reservoir caused the mafic magma to interact with the two distinct zones differently, forming MME in the lower granite and homogeneous hybrid rocks in the upper portion. The plagioclase compositions of the larger MME, smaller MME, hybrid rocks, and granitic host rocks vary between An_{41}–An_{47}, An_{34}–An_{44}, An_{02}–An_{52}, and An_{03}–An_{29} respectively. The alkali feldspar compositions of the hybrid rocks range from Or_{84} to Or_{97}, while that of the host granite varies from Or_{92} to Or_{96}. The biotite is eastonitic and siderophyllitic in composition, while the pyroxene is diopside. The apparent pressure range of biotite crystallization in the granitic rocks was calculated at 1.93 to 2.28 kbar, while the biotite crystallization temperature for the different rock types is in the range of 628 and 759 °C. Oxygen fugacity estimates from the biotite suggest that the Kathalguri magmas crystallized at fO_2 conditions above the nickel-nickel oxide (NNO) buffer. Distinct disequilibrium textures indicating mixing and mingling between the mafic and felsic magmas are preserved in the smaller MME and homogeneous hybrid rocks. These textures are mainly found in plagioclase crystals, which include resorbed grains, oscillatory zoned plagioclase, boxy-cellular morphology, and overgrowth texture. Some common magma mingling and mixing textures like quartz ocelli and back-veining are also preserved in the smaller MME. An interesting feature observed in the homogeneous hybrid rocks of our study area is mantled alkali feldspar in which orthoclase is mantled by microcline. We propose that this overgrowth texture formed due to epitaxial crystallization of microcline on orthoclase owing to mixing between the felsic and mafic magmas. Such magma mixing event produces a heterogeneous system that is in an extreme state of disequilibrium and facilitates the epitaxial growth of one feldspar on another. On the other hand, the larger MME of our study domain shows limited interaction with the felsic host as indicated by the replacement of clinopyroxene crystals by amphibole and biotite.

Keywords Mafic magmatic enclaves · Hybrid rocks · Orthoclase-microcline transformation · Shillong Group, Kathalguri pluton

✉ Bibhuti Gogoi
bibhuti.gogoi.baruah@gmail.com

[1] Department of Geology, Cotton University, Guwahati, Assam 781001, India

[2] Inter University Accelerator Centre, New Delhi 110067, India

1 Introduction

The mixing of diverse magmas has been extensively documented in numerous magmatic domains. Magma mixing is a process, where two compositionally distinct magmas associate to form a homogeneous product of intermediate composition. In many instances, mixing leads to the formation of a heterogeneous product in which the interacting magmas could be identified in the hybrid rock samples and is widely referred to as magma mingling. Mixing is initiated when any particle of one magma is brought closer to the other (Snyder 1997). Thus, for two magmas to mix, they must be mechanically stretched and folded to decrease the distance and increase the surface area of contact between them leading to an increased probability of chemical diffusion (Ottino 1989; Aref and El Naschie 1995). Even though magma mixing is a conventional mechanism, understanding the physical and chemical processes associated with magma interactions and their influence on magmatic systems is still an ongoing process (Perugini and Poli 2012; Sosa-Ceballos et al. 2012; Farner et al. 2014; Gogoi et al. 2020a). Many pieces of literature have suggested that the mixing of magmas can play a vital role in both of diversification of composition in igneous rocks (Blundy and Sparks 1992; Wiebe 1994; De Campos et al. 2004) and triggering of highly explosive volcanic eruptions (Sparks et al. 1977; Snyder 1997; Murphy et al. 1998; Leonard et al. 2002). In addition, the mixing of two disparate magmas offers significant insight into the understanding of the evolutionary history of magma chambers (Huppert et al. 1982; Gogoi et al. 2018; Gogoi and Chauhan 2021). A variety of magma chambers has already been documented from different tectonic settings (Hilderth 1981; Gianetti and Luhr 1983; Wolff and Storey 1984; Worner and Schimincke 1984; Bacon and Druitt 1988; Wolff et al. 1990). Several studies have already suggested that magma chambers may be internally zoned and have distinct rheological boundaries, whose occurrence is primarily attributed to variations in crystallinity of magma (Hildreth and Wilson 2007; Takahashi and Nakagawa 2012; Singer et al. 2014; Gogoi et al. 2018). Thus, the zoned structure in a magma chamber may be formed by fractional crystallization. The internal structure of a magma chamber can be estimated from the differential nature of the eruptive products from a single eruption cycle (Takahashi and Nakagawa 2012) or through geophysical methods like seismic tomography (Romero et al. 1993; Tizzani et al. 2009) or by studying fossilized magma chambers that preserve evidence of magma mixing (Wada et al. 2004; Slaby and Martin 2008; Gogoi et al. 2018; Domańska-Siuda et al. 2019; Gogoi and Chauhan 2021).

Magma mixing also influences the development of disequilibrium textures from megascopic to microscopic scale (Hibbard 1981; Baxter and Feely 2002; Grogan 2002). The primary objective of our research is to elucidate the role of textures depicted by feldspars in a magma mixing environment. The study of igneous feldspars is rewarding since the composition of the crystals in the mixing system depends on the physical and chemical environment existing at the time of their formation. As they commonly occur in both the resident and the invasive magma in felsic-mafic mixing systems, they provide much information about mixing processes. Thus, the composition and textures of feldspars can give an insight into where and when in the magmatic evolution the mineral was originally formed. It also provides information about the conditions during the mixing event (Anderson 1984; Slaby and Götze 2004; Slaby et al. 2008; Pietranik and Koepke 2009; Gogoi and Saikia 2018). Various textures of the feldspar minerals reflect a complex scenario of mixing within the magma chamber in which the crystals form. Textural evidence in the form of resorbed feldspars, sieve texture, compositional zoning, boxy cellular morphology, and overgrowth texture indicates interaction of felsic and mafic magmas (Tepley 1999). Feldspar is an abundant component in igneous rocks, having the great capability in providing progressive records of magma chamber dynamics (Anderson 1983; Stamatelopoulou-Seymour et al. 1990; Blundy and Shimizu 1991; Singer et al. 1995). Its chemistry and crystal habit provides important information regarding the petrogenetic histories of magmatic systems. It is important to note that, feldspar does not disintegrate; instead it equilibrates with the changing environment and persists as a stable crystallizing phase. Hence, the composition and growth morphology of igneous feldspars give a reliable record of the crystallization environment and dynamics of the melt (Anderson 1984).

This paper precisely discusses the field and petrographical observations carried out on the Kathalguri Pluton. This pluton preserves a variety of textural features, which resulted from the mixing and mingling of an invading mafic magma with the felsic host. Emphasis is placed on the compositional and textural analysis of feldspars in the felsic, mafic, and intermediate rocks. Our study possibly documents the first appraisal of magma mixing events in the Mikir Massif. This work has been carried out in one of the least investigated terrains of Precambrian India such that our findings may yield significant insights in understanding the petrogenetic and geotectonic evolution of the Proterozoic Shillong Basin.

2 Geological setting

The Kathalguri Pluton is a part of the igneous intrusives in the Shillong Group of Rocks of the Mikir Hills Massif. The Mikir Massif is the easternmost extension of the Assam-Meghalaya Gneissic Complex (Fig. 1).

2.1 Assam-Meghalaya gneissic complex

The Assam-Meghalaya Gneissic Complex covers an area of about 25,000 km^2, which is the sole representative of Precambrian rocks in northeast India and is separated from the Indian Peninsula by the Garo-Rajmahal Graben. The gneissic complex is restricted primarily in Meghalaya and partly in Karbi Anglong district and a few other districts of Assam. The Precambrian rocks are exposed mainly in three areas: i) Meghalaya Plateau, ii) Mikir Massif and iii) isolated inselbergs in the Brahmaputra valley in Goalpara, Bongaigaon, Dhubri, Kamrup, Darrang, and Sonitpur districts of Assam.

2.2 Mikir Massif

The Mikir Massif is a segment of the Precambrian Assam-Meghalaya Gneissic Complex, which is separated from the Shillong plateau by a major N-S fracture zone viz. Kopili rift. The Mikir Hills Massif spans over an area of about 7000 km^2 within 25.5°–27°N latitude and 92.5°–94°E longitude, forming a horst amidst the vast alluvial tract of middle Assam. The rocks of Mikir Hills Massif are characterized by Proterozoic basement granite gneisses, Mesoproterozoic metasedimentary rocks, granites, migmatites, granulites, Cambrian granites, and Mesozoic-Tertiary igneous and sedimentary rocks (Mazumder 1986; Nandy 2001; Chatterjee et al. 2011; Kumar et al. 2017). The basement gneisses along with the metasedimentary sequence had been intruded by various felsic and mafic igneous rocks, which are indicative of different tectonothermal events.

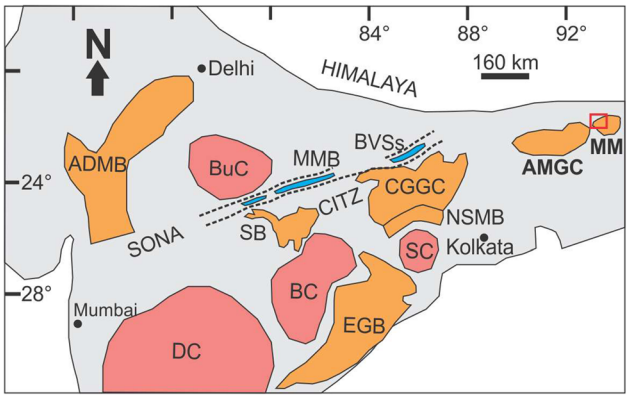

Fig. 1 A simplified geological map of India showing the locations of Assam-Meghalaya Gneissic Complex (AMGC) and Mikir Massif (MM) in the tectonic framework of the Archean cratons and Proterozoic mobile belts (modified after Chatterjee and Ghose 2011). The locality of the Kathalguri Pluton is shown by the red box. Archean cratonic blocks: Bastar Craton (BC), Bundelkhand Craton (BuC), Dharwar Craton (DC), Singhbhum Craton (SC); Proterozoic mobile belts: Aravalli Delhi Mobile Belt (ADMB), Bathani volcano-sedimentary sequence (BVSs), Central India Tectonic Zone (CITZ), Chotanagpur Granite Gneiss Complex (CGGC), Eastern Ghats Belt (EGB), Mahakoshal Mobile Belt (MMB), North Singhbhum Mobile Belt (NSMB), Satpura Belt (SB), Son-Narmada graben (SONA)

2.3 Shillong Group

The Mesoproterozoic Shillong Basin is characterized by a metasedimentary sequence known as the Shillong Group of rocks that form a part of the Shillong Plateau and Mikir Hills. The Shillong Group of rocks unconformably overlies the Basement Gneissic Complex and mainly comprises metavolcanics and metasediments, which is further divided into the Upper and Lower Shillong formation. Upper Shillong Group consists mainly of quartzites intercalated with phyllite and conglomerate. The Lower Shillong Formation is also known as Barapani Formation (Ahmed 1981) comprises mainly of carbonaceous phyllite, thin quartzite layers, slate, conglomerate, and schists with calcsilicate rocks. Neoproterozoic, as well as Cambrian granitic intrusives, are widely distributed within the Shillong Group of rocks.

2.4 Kathalguri pluton

The Kathalguri Pluton is a granite magmatic pluton related to the Pan African orogeny (Majumdar and Dutta 2016; Dhurandhar et al. 2019). This granitic pluton occurs as an intrusive body in the metasedimentary sequence, viz.,

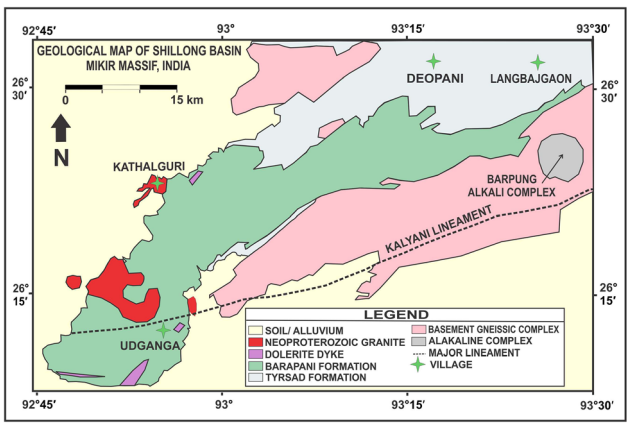

Fig. 2 Regional geological map illustrating the Shillong Group of rocks in the Mikir Massif, Assam (modified after Dhurandhar et al. 2019)

Shillong Group of rocks (Fig. 2). During the crystallization history of the magma chamber, the pluton was intruded by mafic magma leading to magma mixing and mingling. The Kathalguri Pluton hosts a significant number of mafic to hybrid enclaves along with xenoliths composed of pure granite. The lower part of the pluton holds many enclaves of various sizes and shapes. On the other hand, the distribution of the enclaves is markedly less in the upper part of the pluton than that of the lower unit.

3 Field relationships

The Kathalguri Pluton is a granitic domain intruded into the Shillong Group of rocks exposed at Kathalguri village in Nagaon district of Assam (Fig. 2). The granitic rocks are coarse to fine-grained as well as leucocratic to mesocratic in nature. Apart from the granitic rocks, the pluton also hosts dark-coloured mafic rocks in the form of mafic magmatic enclaves (MME) and flows (Fig. 3a–c). Moreover, grey-colored hybrid rocks of intermediate composition are also observed in addition to the granitic and mafic rocks (Fig. 3d). Hand samples representing the different varieties of rocks encountered in our study domain are illustrated in Fig. 4.

The mafic enclaves that are embedded within the granitic rocks are mesocratic to melanocratic and heterogeneously distributed throughout the pluton. The enclaves exhibit both sharp and diffusive contact with the host granitic rocks. Extensive amounts of mafic enclaves are found scattered in the lower part of the pluton. On the other hand, the enclaves are found to be very scarcely distributed in the upper part (Fig. 3a). These enclaves are broadly categorized into two types: (i) larger enclaves, which are dominantly melanocratic and angular in shape (Fig. 3b). The melanocratic nature of these enclaves indicates that they had very limited interaction with the granitic host (ii) smaller enclaves, which display both angular and rounded morphology (Fig. 3a). These enclaves are mesocratic to melanocratic in nature suggesting variable degrees of interaction with the felsic host.

Along with the mafic enclaves, some mafic flows are also observed in the study area. These mafic flows are notably mesocratic in nature. Along with the contacts between the mafic flows and granites, reaction surfaces are remarkably distinct. The reaction surfaces indicate the interaction of the mafic flows with the host granite (Fig. 3c).

The distinct textual evidence in the form of quartz ocelli and back-veining was observed in the lower section of the pluton. The quartz ocelli consist of quartz crystals, which are encircled by mafic minerals such as biotite and/or hornblende (Fig. 3e). These ocelli were encountered in the mafic enclaves of the study area which are transforming into hybrids due to their interaction with the felsic host. The quartz crystals forming ocelli were incorporated in the mafic hybrid magma from the felsic system, in an environment where they were unstable and in due course leading to the development of clusters of quartz crystals consisting of mafic rims (Vernon 1990; Hibbard 1991; Baxter and Feely 2002). Some outcrops display intrusion of granitic veins into the mafic enclaves, which infers back veining (Fig. 3f). This feature is indicative of interaction between the invading mafic magma and the host granite. During the mixing of felsic and mafic magmas, the initial temperature difference between the two different magma types is relatively large. This facilitates the mafic magma to superheat its felsic counterpart and significantly decrease the viscosity of the latter enabling it to back-vein the mafic material (Blake 1981; Vernon et al. 1988).

4 Petrography

Petrographical observations are broadly carried out in three different rock types of the Kathalguri Pluton: (i) mafic rocks, represented by larger mafic enclaves that are melanocratic in nature and appear closest in composition to the invasive mafic magma. These mafic rocks appear to have been least modified by the felsic host; (ii) granite, representing the felsic magma; (iii) hybrid rocks, representing products of felsic-mafic magma interactions. Two distinct types of hybrid rocks are observed in the form of smaller mafic enclaves and gray-coloured intermediate rocks that are homogeneous. These hybrids indicate varying degrees of interaction between the invading mafic magma and felsic host.

4.1 Mafic rocks

Samples collected from the larger mafic enclaves consist of mineral grains, which are mostly anhedral in shape representing allotriomorphic texture. These rocks are holocrystalline. The major constituent phases found in these enclaves are pyroxene, biotite, plagioclase, amphibole, and iron oxide. Few of the pyroxene crystals are mantled by amphibole and biotite suggesting that the latter were produced at the expense of the former (Fig. 5a).

4.2 Granite

The granite samples are medium to coarse-grained with the mineral grains ranging from subhedral to anhedral in shape. These rocks consist of major mineral phases such as biotite, plagioclase, alkali feldspar, quartz with epidote, muscovite,

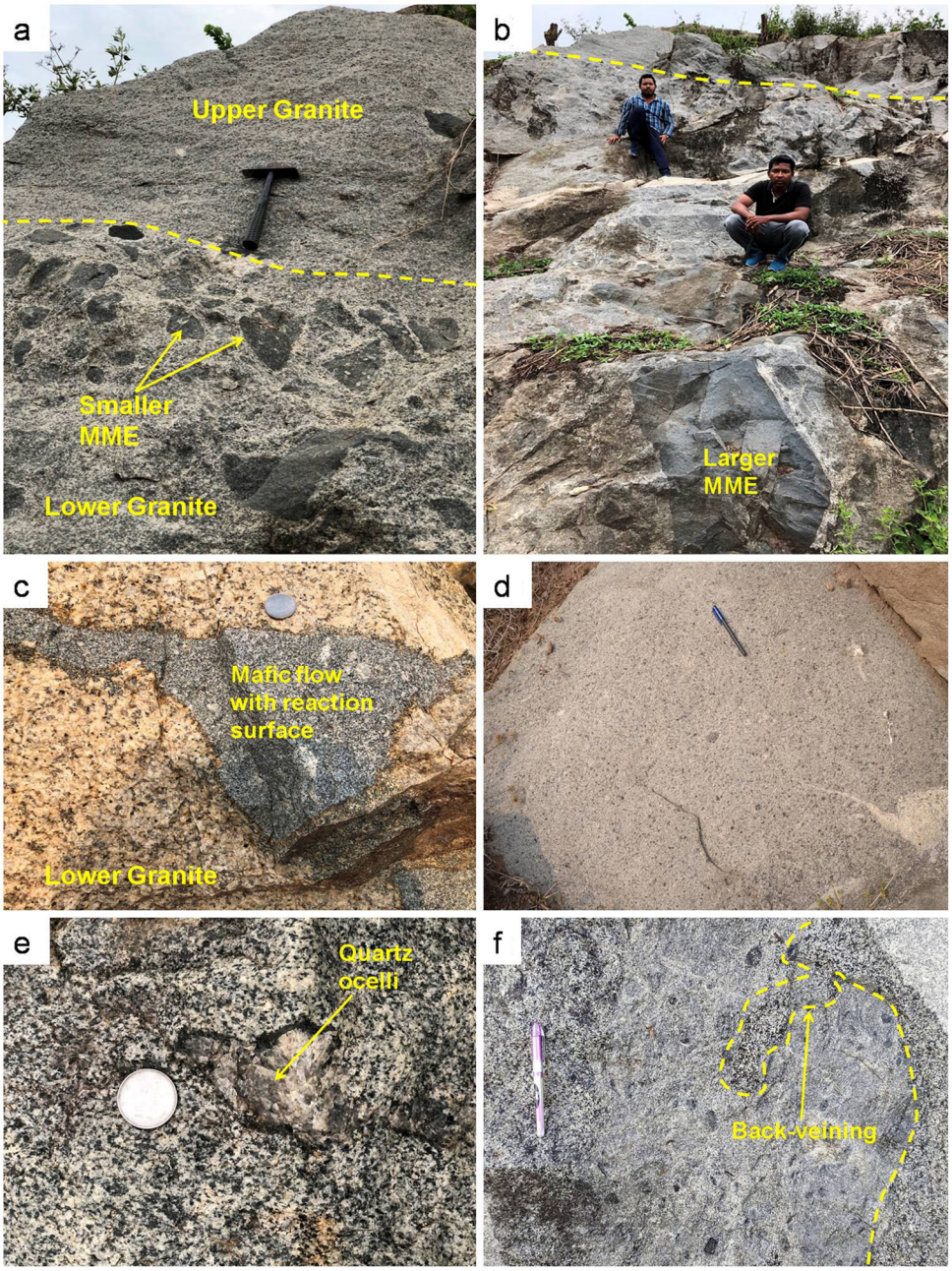

Fig. 3 Field photographs displaying **a** Contact between the upper and lower granites demarcated by the yellow dashed line. The mafic magmatic enclaves are widely distributed in the lower granite **b** A larger mafic enclave preserved in the lower granite. The contact between the upper and lower granites is shown by the yellow dashed line **c** Mafic flow in the lower granite. Well-defined reaction surface can be seen at the mafic-felsic contact **d** Homogeneous hybrid rock **e** Quartz ocelli **f** Back-veining

titanite, apatite, zircon, and iron oxide as minor constituents.

The granitic samples show holocrystalline and allotriomorphic texture. In some plagioclase crystals, intergrowth of branching rods of quartz is observed depicting myrmekitic texture. Such quartz intergrowths are also observed in some alkali feldspar grains representing graphic texture. Moreover, irregular lamellae of plagioclase within some alkali feldspar grains are also seen depicting perthitic texture (Fig. 5b).

4.3 Hybrid rocks

The hybrid rock samples consisting of smaller mafic enclaves and intermediate rocks have similar mineralogical and textural assemblages. The constituent mineral phases found in these rocks include plagioclase, alkali feldspar, biotite, quartz, amphibole, apatite, chlorite, titanite, and iron oxide.

Distinct disequilibrium textures indicating mixing and mingling between the mafic and felsic magmas are seen in the hybrid rocks. These textures are mainly found in plagioclase crystals, which are subhedral to anhedral in shape.

Fig. 4 Hand samples representing **a** Coarse-grained lower granite **b** Fine-grained upper granite **c, d** Homogeneous hybrid rocks **e** Smaller mafic enclave **f** Larger mafic enclave

Several textures like resorbed grains, oscillatory zoned plagioclase, boxy-cellular morphology, and overgrowth texture are observed in the plagioclase crystals. One of the most vital petrographic features observed in these rocks is the presence of resorbed crystals of plagioclase showing rounded morphology (Figs. 5c, d). The mineral also shows oscillatory zoning patterns indicating variations in compositional amplitudes at regular intervals within such crystals (Fig. 5e). Oscillatory zoned plagioclase crystals are characterized by zones of varying thickness ranging from 10 to 100 µm. Boxy-cellular morphology with box-like cells having partially resorbed edges is also seen (Fig. 5f). Some of the plagioclase crystals are embayed by distinct, strong normally zoned overgrowth rims. These rims are a few tens of microns thick and tend to reinstate the euhedral boundary of the crystal (Fig. 5g).

Another interesting feature observed in the intermediate hybrid rocks is the overgrowth of microcline on orthoclase feldspar. The presence of this feature represents epitaxial crystallization of microcline on orthoclase crystals. The transition between orthoclase and microcline is sharp, while the inner orthoclase displays perthitic texture (Figs. 5h, i).

5 Analytical methods

The mineral composition was determined with the Electron Probe Micro Analyzer (EPMA) CAMECA SXFive instrument at DST-SERB National Facility, Department of Geology (Center of Advanced Study), Institute of Science, Banaras Hindu University. Polished thin sections were

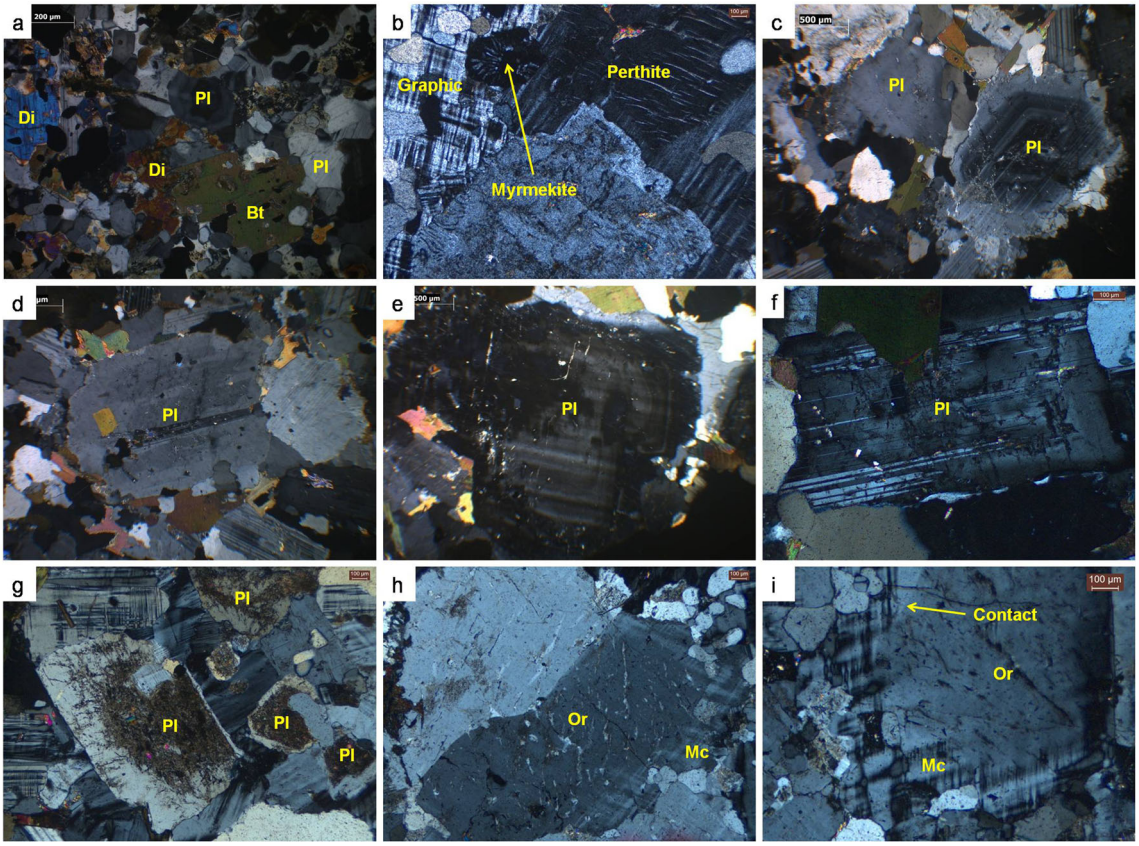

Fig. 5 Photomicrographs displaying **a** Association of pyroxene and biotite in the larger mafic enclaves or mafic rocks **b** Graphic, myrmekite and perthitic texture preserved in the granitic rocks **c, d** Resorbed plagioclase grains in the hybrid rocks **e** Oscillatory zoning in plagioclase **f** Boxy-cellular plagioclase **g** Sieve-textured plagioclase crystals with normally zoned overgrowth rims **h, i** Mantling of perthitic orthoclase by microcline. Mineral abbreviations: Bt = Biotite, Di = Diopside, Mc = Microcline, Or = Orthoclase, and Pl = Plagioclase

coated with a 20 nm thin layer of carbon for electron probe micro analyses using the LEICA-EM ACE200 instrument. The CAMECA SXFive instrument was operated by SXFive Software at a voltage of 15 kV and 10 nA current with a LaB_6 source in the electron gun for the generation of an electron beam. The natural silicate mineral andradite was used as an internal standard to verify the positions of crystals (SP1-TAP, SP2-LiF, SP3-LPET, SP4-LTAP, and SP5-PET) to corresponding wavelength dispersive (WD) spectrometers (SP). The following X-ray lines were used in the analyses: F-Kα, Na-Kα, Mg-Kα, Al-Kα, Si-Kα, P-Kα, Cl-Kα, K-Kα, Ca-Kα, Ti-Kα, Cr-Kα, Mn-Kα and Fe-Kα. Natural mineral standards fluorite, halite, apatite, periclase, corundum, wollastonite, orthoclase, rutile, chromite, rhodonite, and hematite standard supplied by CAMECA-AMETEK were used for routine calibration, X-ray elemental mapping, and quantification. Routine calibration, quantification, acquisition, and data processing were carried out using SxSAB version 6.1 and SX-Results software of CAMECA. The precision of the analysis is better than 1% for major element oxides and the error on trace elements concentrations varied between 3 and 5% based on repeated analysis of standards (Chauhan et al. 2020; Gogoi et al. 2021).

6 Mineral chemistry

6.1 Plagioclase

Plagioclase occurs as a major mineral phase in all the different rock types of our study area. Representative EPMA analytical data of plagioclase occurring in the larger mafic enclaves of Kathalguri Pluton are given in Supplementary Table 1. Altogether eight single-point analyses of individual plagioclase grains from the sample MM4 are reported. The analyzed data of plagioclase plots in the field of andesine (Fig. 6a) with An content ranging from An_{41} to An_{47}.

Altogether seven single-point analyses of individual plagioclase grains were carried out in sample MF6 representing the granitic rocks. The representative data of plagioclase from the granite sample are given in Supplementary Table 2. Here, plagioclase compositions

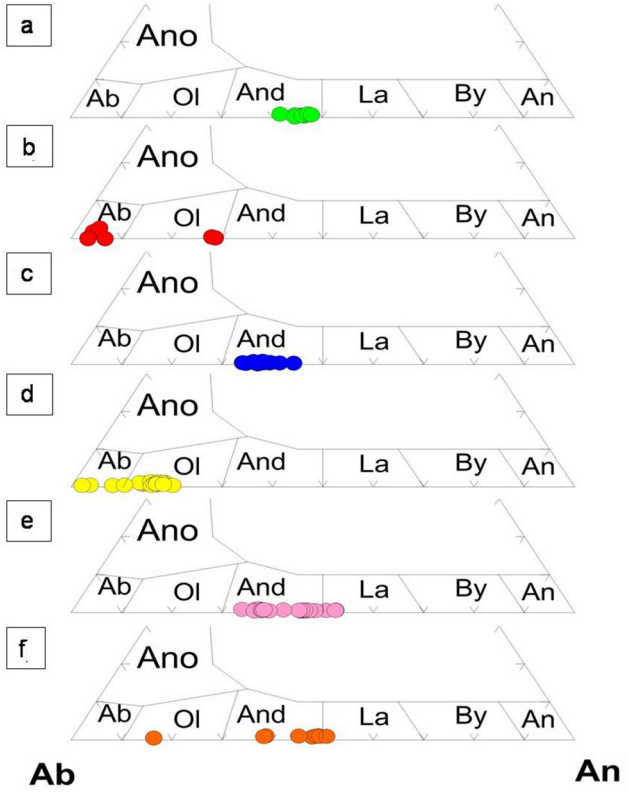

Fig. 6 Nomenclature of plagioclase occurring in the **a** Larger mafic enclaves **b** Granitic rocks **c** Smaller mafic enclaves **d, e, f** Homogeneous hybrid rocks

plot in the fields of albite and oligoclase (Fig. 6b) with An content ranging from An_3 to An_{29}.

Core-rim analyses of plagioclase grains were carried out in the hybrid rocks, which include smaller mafic enclaves and homogeneous intermediate rocks. Three samples, viz. MF8, MF16, and MH9 were analyzed from the intermediate rocks, while one sample, viz. MM1 was analyzed from the smaller mafic enclaves. Core-rim analyses (Supplementary Table 3) were carried out in a single oscillatory zoned plagioclase crystal of sample MM1 plot in the field of andesine (Fig. 6c). The analyzed plagioclase grain clearly shows oscillatory zoning illustrated by many distinct calcic spikes (Fig. 7a). Such calcic spikes in plagioclase serve as strong evidence of magma mixing (Hibbard 1991; Baxter and Feely 2002; Gogoi and Chauhan 2021). On the other hand, the analytical data of two plagioclase grains from the sample MF8 (Supplementary Table 4) plot in the fields of albite and oligoclase (Fig. 6d). The compositions of three plagioclase grains are plotted in the fields of andesine and labradorite (Fig. 6e) for the sample MF16 (Supplementary Table 5). Furthermore, compositions of one plagioclase grain from the sample MH9 (Supplementary Table 6) plot in the fields of oligoclase, andesine, and labradorite (Fig. 6f). The core-rim analyses of plagioclase from the three samples representing the homogeneous intermediate rocks show an overall normal zoning pattern with less pronounced calcic spikes (Fig. 7b–g). Of particular importance are the plagioclase analyses of sample MF8 that display a pronounced calcic spike towards the rim followed by a strongly normally zoned rim (Fig. 7c, d). Such strongly normally zoned rims over partially resorbed plagioclase crystals have been reported from other magma mixing scenarios (Tepley et al. 1999).

6.2 Alkali feldspar

Representative EPMA analyses of alkali feldspar were carried out in the granitic as well as homogeneous intermediate rocks of Kathalguri Pluton. This mineral is not found in the larger mafic enclaves of our study area. A total of eight single-point analyses were obtained from individual alkali feldspar grains occurring in the granite sample MF6 (Supplementary Table 7). Here, the alkali feldspar compositions plot in the field of orthoclase (Fig. 8a) with Or content ranging from Or_{92} to Or_{96}. Consequently, core-rim analyses were obtained from alkali feldspar grains occurring in the homogeneous hybrid rock samples, viz. MF8, MF16, and MH11. The analytical data of alkali feldspar from the three hybrid samples are provided in Supplementary Tables 8, 9, and 10. The alkali feldspars from the three samples show similar compositions and plots in the field of orthoclase (Figs. 8b–d). Moreover, the presence of orthoclase-microcline transformation in the sample MH11 does not have any influence on the overall feldspar composition, i.e., the orthoclase-microcline transition is not characterized by any marked compositional change.

6.3 Pyroxene

Representative data of pyroxene from the larger mafic enclaves (sample MM4) are reported in Supplementary Table 11. A total of ten data points were analyzed from individual pyroxene grains present in MM4. The pyroxene formula was calculated based on six oxygen atoms (Morimoto et al. 1988) and the entire pyroxene data plot in the field of diopside (Fig. 9).

6.4 Biotite

It is present as a major mineral phase in all the different varieties of rocks of our study area. Biotite compositions were determined from each of the vivid rock types to understand the magma mixing process in the Kathalguri Pluton. The biotite endmember calculation was performed based on 22 oxygen atoms and Fe^{2+}–Fe^{3+} segregation of

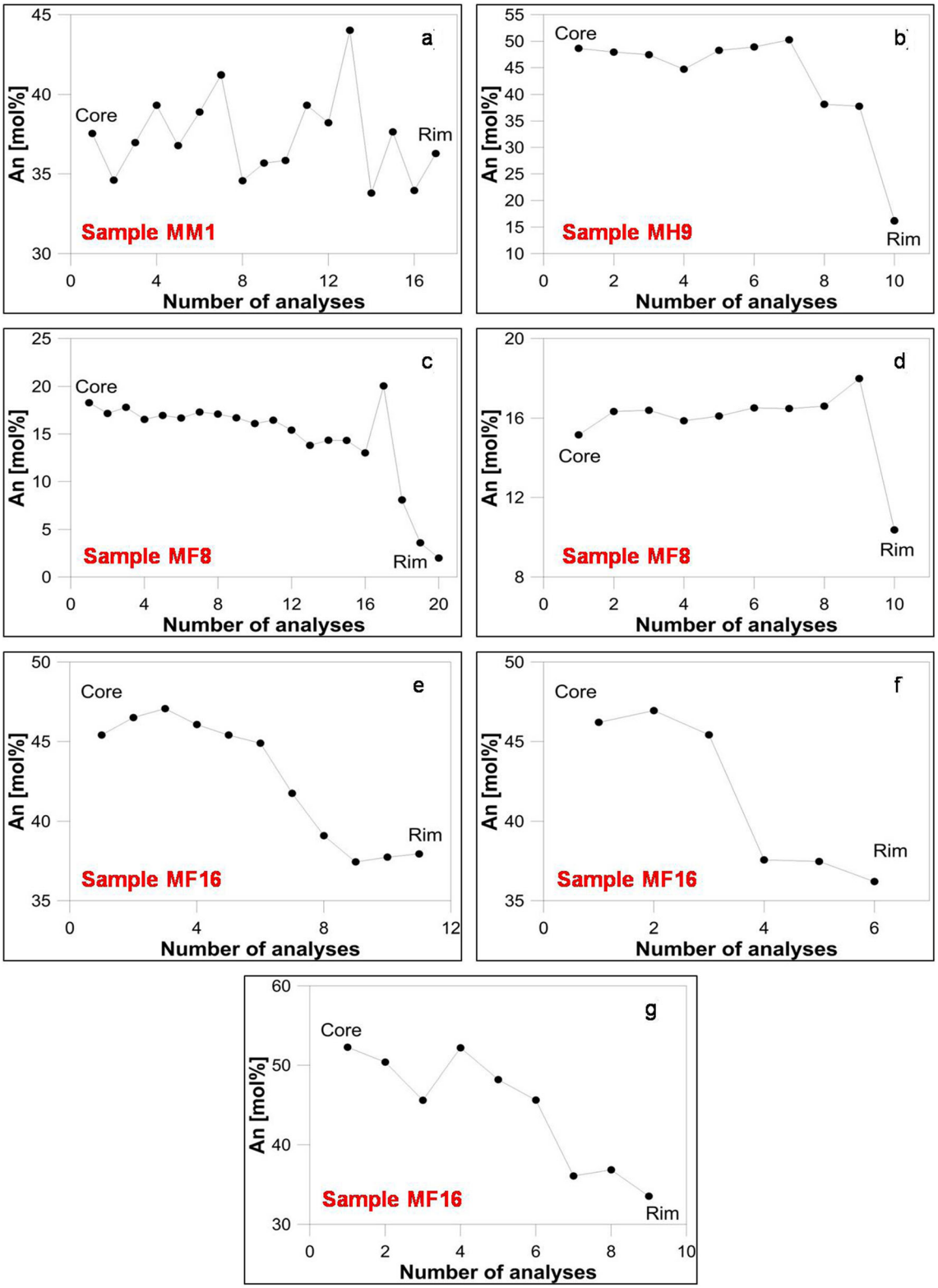

Fig. 7 Core-rim analyses of plagioclase showing anorthite content in mol% from the **a** Smaller mafic enclaves **b, c, d, e, f, g** Homogeneous hybrid rocks

total iron content (FeO_t) was done using the charge balance procedure of Dymek (1983).

Representative EPMA analyses of biotite from the mafic rocks or larger mafic enclaves (Sample MM4) are presented

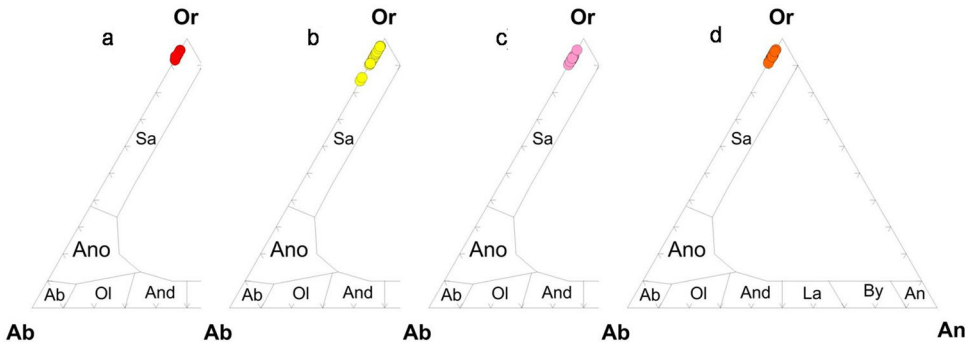

Fig. 8 Nomenclature of alkali feldspar occurring in the **a** Granitic rocks **b, c, d** Homogeneous hybrid rocks

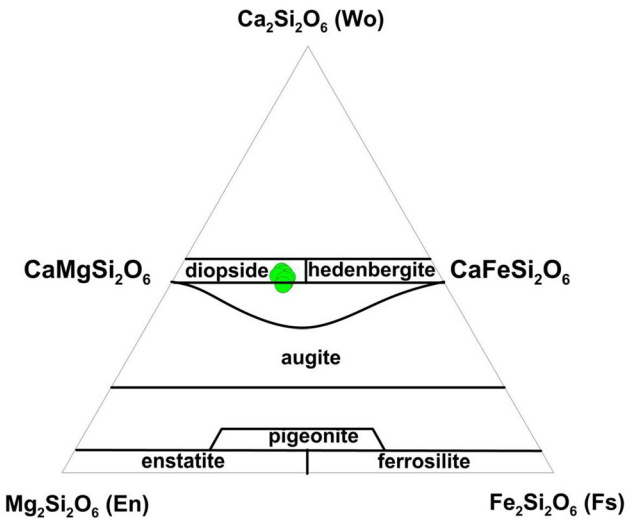

Fig. 9 Ca–Mg–Fe pyroxene classification plot displaying the composition of clinopyroxene from the larger mafic enclaves

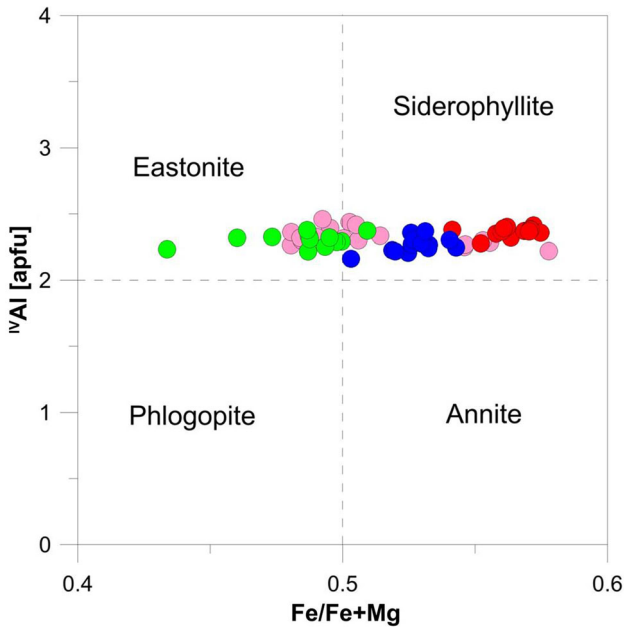

Fig. 10 Al^{iv} vs. Fe/Fe + Mg classification plot showing the composition of biotite from the mafic, felsic, and hybrid rocks of the Kathalguri Pluton. Colors represent: green = mafic rocks or larger mafic enclaves, red = granitic rocks, blue = smaller mafic enclaves, and pink = homogeneous hybrid rocks

in Supplementary Table 12. Biotite from this particular rock plots in the fields of eastonite and siderophyllite (Fig. 10). On the other hand, biotite compositions from the felsic or granitic rocks (Sample MF6) cluster in the region of siderophyllite (Fig. 10; Supplementary Table 13). Meanwhile, biotite analyses were also carried out in the smaller mafic enclaves (Sample MM1; Supplementary Table 14) and homogeneous hybrid rocks (Samples MH11 and MF16; Supplementary Table 15). On the Al^{iv} vs. Fe/Fe + Mg classification plot (Speer 1984), biotite from the smaller mafic enclaves clusters in the field of siderophyllite, while those from the homogeneous hybrid rocks range in composition from siderophyllite to eastonite (Fig. 10). Overall, the compositions of biotite from the smaller enclaves and homogeneous hybrids plot within the compositional domain of the felsic and mafic biotites forming a continuous linear trend, which suggests the role of magma mixing in the studied pluton. Moreover, in the Mg vs. Fe/Fe + Mg and Fe vs. Fe/Fe + Mg plots (Fig. 11a, b), compositions of biotite from the mafic, felsic, and hybrid rocks display linear trends. Biotite occurring in the granite is Fe-rich, while those occurring in the larger mafic enclaves are Mg-rich. The compositions of biotite from the smaller mafic enclaves and homogeneous hybrid rocks fall within the Mg- and Fe-rich biotites and their Mg–Fe abundances vary linearly. Such signatures suggest the rocks under investigation have been affected by magma mixing (Gogoi et al. 2020b).

7 Discussion

7.1 Crystallization conditions of the Kathalguri pluton

7.1.1 Temperature and oxygen fugacity

The crystallization temperature of biotite can be estimated from its Ti content and X_{Mg} values. The Ti contents of

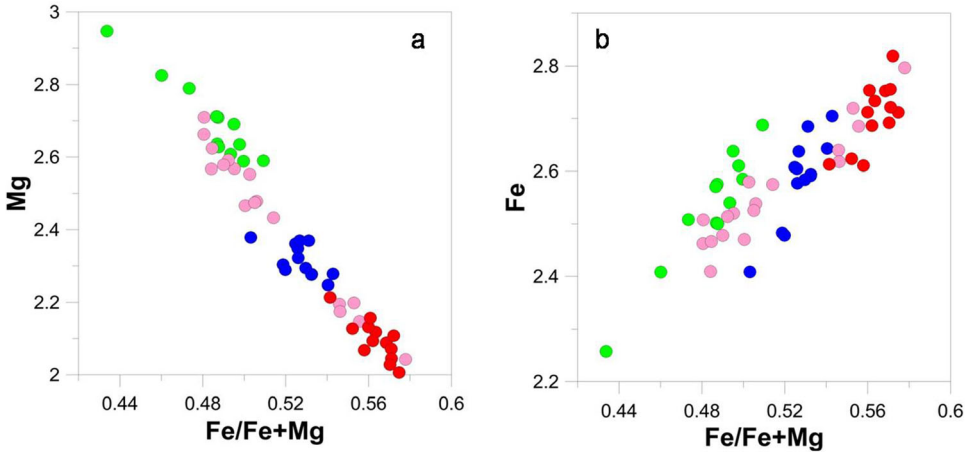

Fig. 11 **a** Mg vs. Fe/Fe + Mg **b** Fe vs. Fe/Fe + Mg plots of biotite. Colors represent: green = mafic rocks or larger mafic enclaves, red = granitic rocks, blue = smaller mafic enclaves, and pink = homogeneous hybrid rocks

biotite from the mafic, felsic, and hybrid rocks were plotted against X_{Mg} values in the Ti vs. Mg/(Mg + Fe) diagram of Henry et al. (2005). Results drawn from the Ti-in-biotite geothermometer suggest that the biotites from the different rock types crystallized at a range of temperatures spanning between 600 and 750 °C (Fig. 12). Biotite crystallization temperatures were also evaluated applying the geothermometer of Luhr et al. (1984). Luhr's thermometer evaluates the crystallization temperature of biotite using the empirical formula

$$T\ (K) = 838/\left(1.0337 - Ti/Fe^{2+}\right) \quad (1)$$

This particular geothermometer estimated the crystallization temperatures of biotite to vary between 628 and 759 °C (Supplementary Tables 12−15). Thus, both the geothermometers give similar biotite crystallization temperatures for the mafic, felsic, and hybrid rocks of the Kathalguri Pluton. It has to be noted here that biotite from the mafic rocks or larger mafic enclaves shows higher crystallization temperatures in comparison to that of the felsic and hybrid rocks (Fig. 12).

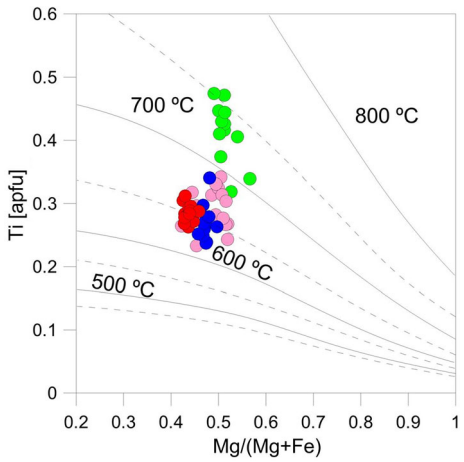

Fig. 12 Ti vs. Mg/(Mg + Fe) plot of biotite from the Kathalguri Pluton (after Henry et al. 2005) showing temperatures of biotite formation. Colors represent: green = mafic rocks or larger mafic enclaves, red = granitic rocks, blue = smaller mafic enclaves, and pink = homogeneous hybrid rocks

Biotite composition can also play an important role to ascertain the oxygen fugacity conditions that existed during magma crystallization. Wones and Eugster (1965) postulated the empirical correlation between biotite composition and oxygen fugacity (fO_2) in their experimental work, thus highlighting the importance of this mineral in redox assessment. The duo proposed an Fe^{3+}–Fe^{2+}–Mg redox assessment plot in which biotite compositions are matched with common oxygen buffers: quartz-fayalite-magnetite (QFM), nickel-nickel oxide (NNO), and hematite-magnetite (HM). The fO_2 of biotite from the mafic, felsic, and hybrid rocks cluster between the NNO and HM buffers (Fig. 13), suggesting an oxidizing environment at the time of crystallization of the mineral.

The oxygen fugacity conditions of crystallization for the mafic, felsic, and hybrid rocks were also ascertained using the Fe/(Fe + Mg) ratio of biotite. The experimental isobaric (2070 bar) fO_2-T plot of Wones and Eugster (1965) illustrates the gradual changes in oxygen fugacity conditions with increasing temperatures. Biotite compositions (100 × Fe/Fe + Mg) projected onto the T-fO_2 plot display crystallization conditions between the NNO and HM buffers for all the biotites of the Kathalguri Pluton (Fig. 14), revealing oxidizing conditions during magma crystallization.

7.1.2 Pressure and depth

Biotite composition can be used to estimate the crystallization pressure of the mineral, which in turn can give us an idea about the emplacement depth of magmas. Uchida et al. (2007) highlighted the empirical correlation between the total Al (Al^T) content of biotite (calculated based on 22 oxygen atoms) and crystallization pressure (P), thus

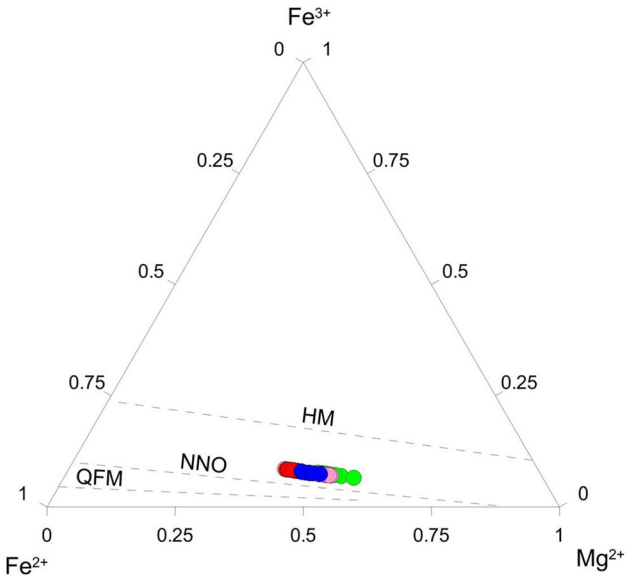

Fig. 13 Variations of Fe^{3+}–Fe^{2+}–Mg^{2+} in biotite from the mafic, felsic and hybrid rocks of the Kathalguri Pluton (after Wones and Eugster 1965). HM, NNO and QFM are the buffer curves for hematite–magnetite, nickel–nickel oxide, and quartz-fayalite-magnetite buffers respectively. Colors represent: green = mafic rocks or larger mafic enclaves, red = granitic rocks, blue = smaller mafic enclaves, and pink = homogeneous hybrid rocks

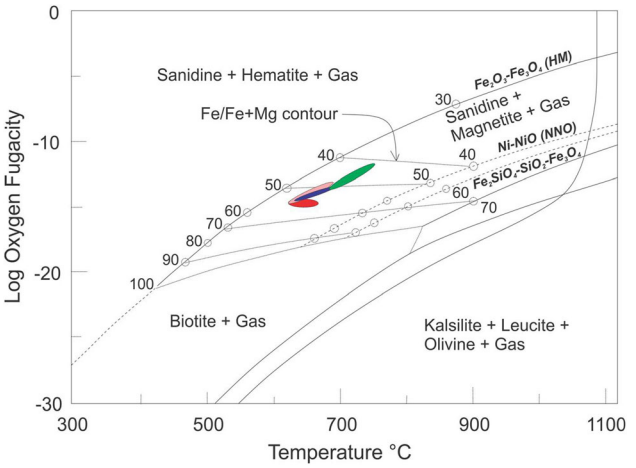

Fig. 14 Log fO_2-T plot based on biotite composition (after Wones and Eugster 1965) showing the redox condition of the mafic, felsic, and hybrid rocks of the Kathalguri Pluton. Colors represent: green = mafic rocks or larger mafic enclaves, red = granitic rocks, blue = smaller mafic enclaves, and pink = homogeneous hybrid rocks

underlining the relevance of this mineral in pressure estimation. They proposed a simple empirical equation that can be used to estimate solidification pressure from biotite composition. The empirical equation can be expressed as:

$$P\ (\text{kbar}) = 3.03 \times Al^{T} - 6.53(\pm 0.33) \quad (2)$$

The pressures evaluated by using the above-mentioned equation range between 1.93 and 2.28 kbar (average = 2.12 kbar; Supplementary Table 13). The average pressure obtained conforms to an emplacement depth of approximately 8 km for the Kathalguri Pluton.

7.2 Magma chamber dynamics involving magma mixing

From field and textural relationships, it is evident that magma mixing played a vital role during the evolution of the felsic magma chamber. The Kathalguri Pluton is a granitic domain that was intruded by mafic magma during its crystallization history. Field evidence of magma mixing like quartz ocelli and back-veining are preserved in the mafic enclaves (Fig. 3e, f), which are heterogeneously distributed throughout the pluton. A good number of mafic enclaves are spotted in the lower part of the pluton (Fig. 3a, b), while the upper part is devoid of such enclaves, which suggests that the felsic magma chamber was vertically zoned when mafic magma intruded it. In all probability, the mafic magma intruded the felsic reservoir from its bottom and ascended through the lower portion of the reservoir, which was in all likelihood crystal-rich, and subsequently broke up into discrete mafic blobs as indicated by widespread distribution of mafic enclaves in the lower granite (Fig. 3a). On the other hand, the mafic magma interacted with the upper portion of the magma chamber, which was in all likelihood crystal-poor, to produce homogeneous hybrid rocks (Fig. 3d). These observations suggest that the Kathalguri Pluton epitomizes a fossilized felsic magma chamber that was vertically zoned as a result of fractional crystallization.

Furthermore, field observations indicate that the larger mafic enclaves are melanocratic in nature and share sharp boundaries with the felsic host (Fig. 3b), while petrographic observations reveal that crystals of clinopyroxene are replaced by amphibole and biotite. These observations suggest that the larger mafic enclaves underwent limited interaction with the host felsic magma, which was presumably restricted to the chemical exchange of elements. Meanwhile, the smaller mafic enclaves appear mesocratic to melanocratic in nature and share sharp to diffused boundaries with the felsic host (Fig. 3a). Petrographical observations have revealed that several feldspar disequilibrium textures are preserved in the smaller enclaves like resorbed grains, oscillatory zoned plagioclase, boxy-cellular morphology, and overgrowth texture (Figs. 5c–g). These textures are also observed in the homogeneous hybrid rocks. These observations suggest that the smaller mafic enclaves underwent higher degrees of interaction with the host granitic magma. It can be concluded from the above discussion that varying degrees of magmatic interaction occurred in the Kathalguri Pluton during its evolution.

7.3 Feldspar disequilibrium assemblage and their implications

The development of disequilibrium textures in plagioclase has been studied in several pieces of literature (Hibbard 1981; Tepley 1999; Castro 2001; Grogan et al. 2002; Temizel 2013). The principal driving force involved in the development of disequilibrium textures in igneous rocks is the physical and chemical interactions of two disparate magmas during the mixing process (Hibbard 1981). The formation of these disequilibrium textures is mainly controlled by diffusion i.e. thermal and chemical diffusion, where chemical diffusion lasts longer than thermal diffusion (Anderson and Eklund 1994; Grogan et al. 2002).

The study of plagioclase feldspar is very significant as they crystallize early and their preservation of disequilibrium textures carries a reliable record of the dynamic magmatic history of igneous rocks. A variety of disequilibrium textures in plagioclase has been observed in the hybrid magmatic rocks of our study area such as resorbed grains, oscillatory zoned plagioclase, boxy-cellular morphology, and overgrowth texture (Figs. 5c–g).

When a hotter mafic magma intrudes into a system where relatively colder felsic magma is crystallizing, thermal quenching of the former and superheating of the latter lead to resorption and dissolution of the crystallizing plagioclases (Hibbard 1981). Moreover, oscillatory zoned plagioclase feldspars are the characteristic feature of many igneous rocks. These zoning patterns document alternating compositional fluctuations across the plagioclase grains with changes in An and Ab contents. Two major zoning patterns have been categorized by Pearce and Kolisnik (1990): (a) Type I zoning, characterized by fine oscillations ranging from 1 to 10 μm in width and An content ranging from 1 to 10 %. These oscillations were formed due to small perturbations in magmatic systems. (b) Type II zoning, characterized by 10–100 μm wide oscillations with An content ranging from 10 to 25 %. These oscillations were formed due to the occurrence of large-scale disturbances in the crystallizing system such as magma mixing. Type II oscillatory zoning has been observed in plagioclases of the smaller mafic enclaves of Kathalguri Pluton. The presence of this feature in the smaller mafic enclaves of our study area suggests higher degrees of interaction between these enclaves and the host felsic magma.

Plagioclase crystals with boxy-cellular morphology are considered to be a result of an effective undercooling. This is caused due to change in the composition of the melt towards a more anorthite-rich composition leading to anorthite oversaturation in a plutonic environment (Castro 2001). In the Kathalguri Pluton, boxy-cellular morphology is reported from the plagioclases of the homogeneous hybrid rocks. Here, the boxy-cellular plagioclases were formed due to oversaturation of anorthite in the felsic magma where plagioclases were crystallizing during the intrusion of the anorthite-rich mafic magma. The mixing of anorthite-rich mafic magma with the crystallizing felsic magma caused the composition of the felsic magma to move towards a more anorthite-rich composition leading to anorthite oversaturation and resulting in the formation of boxy-cellular morphology in some of the crystallizing plagioclases.

Furthermore, overgrowth textures shown by plagioclase feldspars are formed either by nucleation or by the dissolution of the pre-existing crystals producing normally zoned rim around the crystals (Streck 2008). Overgrowth rim existing around the resorbed plagioclase crystals tends to restore the euhedral outline that reflects retainment of equilibrium conditions (Tepley 1999). Distinct normally zoned rims in resorbed plagioclase crystals were observed in the homogeneous hybrid rocks. The occurrence of such a feature indicates that the plagioclases crystallizing in the felsic magma underwent dissolution when hotter mafic magma invaded the colder felsic magma.

Another interesting disequilibrium texture shown by feldspars is the overgrowth of microcline on orthoclase (Figs. 5h, i). Overgrowth of microcline on amazonite has been discussed by Blasi et al. (1984). The transformation from orthoclase to microcline is facilitated by solution-redeposition processes due to the infiltration of fluid at near-surface temperature. At a temperature less than 500 °C, the release of strain energy in perthite lamellar boundaries and twin-domain walls of feldspars, followed by Si, Al ordering, provides the driving forces for dissolution and redeposition of more ordered phases (Waldron et al. 1993). Worden et al. (1990) proposed that the driving force for dissolution during perthite coarsening leads to the decrease in total free energy due to the release of elastic strain energy in coherent cryptoperthites, coupled with a decrease of perthite interfacial energy on coarsening. There is no such role of compositional changes in orthoclase-microcline transformation but decrease in total free energy by releasing of strain energy present in the orthoclase and increasing Si, Al order in the newly formed microcline (Brown and Parsons 1989). Thus, the low-temperature reactivity of many feldspars associated with aqueous fluid can be attributed to stored energy present in the microtextures resulting from the processes not accomplished at high temperatures. Our present study provides new insights into the present understanding of mantled feldspars. Here, we propose that the mantled alkali feldspars were produced due to epitaxial crystallization of microcline on orthoclase owing to mixing between the felsic and mafic magmas. Such magma mixing event produces a heterogeneous hybrid system that is in an extreme state of disequilibrium. When a hotter mafic magma intrudes into a crystallizing

felsic system, thermal quenching of the former and superheating of the latter lead to resorption and dissolution of the crystallizing feldspars (Hibbard 1981). The orthoclase crystals in the mantled alkali feldspars were crystallizing in the felsic magma chamber when mafic magma intruded it and, in all probability, this event halted the crystallization of orthoclase and further drove its resorption. In the meantime, new phases began to crystallize in equilibrium with the hybrid magma. A late-stage residual aqueous fluid left over from the crystallization of the hybrid magma took the resorbed orthoclase crystals as nuclei and induced epitaxial crystallization of microcline on orthoclase to produce the mantled alkali feldspars. However, more such mantled alkali feldspars have to be reported from other magma mixing scenarios to validate our hypothesis.

Based on petrographical observations and mineral chemical analyses, we infer that varying degrees of interaction between intrusive mafic and host felsic magmas occurred in the Kathalguri Pluton. The hybrid rocks, viz. smaller mafic enclaves and homogeneous hybrids of our study display a wide range of disequilibrium textures in the plagioclase feldspars. From mineral chemical analyses, it is evident that the plagioclase grains of the smaller mafic enclaves and homogeneous hybrids show distinct compositional discontinuities or calcic spikes. The numerous calcic spikes from core to rim shown by the plagioclase grains of the smaller mafic enclaves are oscillatory suggesting extensive magma mixing. On the other hand, the plagioclase grains from the homogeneous hybrid rocks show overall normal zoning with less pronounced calcic spikes from core to rim. Although plagioclase grains from the mafic rocks, viz. larger mafic enclaves are devoid of disequilibrium textures, alteration of pyroxene to amphibole and biotite indicates a lesser degree of interaction between the two magmatic phases. However, disequilibrium textures are absent in the plagioclase crystals of the granitic rocks, which suggests that they were least modified by the magma mixing processes.

8 Conclusions

The Kathalguri Pluton was a vertically zoned granitic magma chamber that was intruded by mafic magma during its crystallization history. In all probability, the lower portion of the granitic magma chamber was occupied by crystal mush while the upper part was dominated by melt when mafic magma intruded it. The invading magma interacted differently with the rheologically distinct upper and lower zones, forming mafic magmatic enclaves in the lower part of the pluton and homogeneous hybrid rocks in the upper region. The mafic enclaves distributed in the lower domain can be broadly divided into two categories: (i) larger enclaves, which are dominantly melanocratic and underwent very limited interaction with the granitic host (ii) smaller enclaves, which are mesocratic to melanocratic in nature and underwent variable degrees of interaction with the felsic host.

Several disequilibrium textures of magma mixing and mingling are preserved in the smaller mafic enclaves and homogeneous hybrid rocks of the Kathalguri Pluton. These textures are mainly showcased by plagioclase crystals, which include resorbed grains, oscillatory zoning, boxy-cellular morphology, and overgrowth texture. Some common magma mingling and mixing textures like quartz ocelli and back-veining are also preserved in the smaller enclaves. An interesting feature observed in the homogeneous hybrid rocks of our study domain is the overgrowth of microcline on orthoclase. We propose that the mantled alkali feldspars were produced by epitaxial crystallization of microcline on orthoclase owing to mixing between the felsic and mafic magmas. On the other hand, the larger mafic enclaves of the Kathalguri Pluton show limited interaction with the host granitic magma as indicated by the replacement of clinopyroxene crystals by amphibole and biotite.

Supplementary Information The online version contains supplementary material available at https://doi.org/10.1007/s11631-022-00534-1.

Acknowledgements We would like to express our sincere gratitude to the anonymous reviewer(s) for their insightful and constructive comments. We thank Managing Editor Dr. Binbin Wang for handling the manuscript. We would also like to thank Professor Ewa Slaby for encouraging us to prepare this manuscript. The authors acknowledge the DST-SERB grant vide Project No. CRG/2020/002635 and CSIR-JRF fellowship No. 09/1236(0005)/2019-EMR-I. The authors are grateful to Professor N.V. Chalapathi Rao for EPMA analyses at DST-SERB National Facility, Department of Geology (Center of Advanced Study), Institute of Science, Banaras Hindu University. The optical photomicrographs were obtained using the microscope-imaging facility established through DST-FIST funding (SR/FST/ESI-152/2016) at the Department of Geological Sciences, Gauhati University.

Declarations

Ethical approval The authors declare that in this present work there is no conflict of interests.

References

Ahmed M (1981) Stratigraphic class of Shillong group, Khasi Hills, Meghalaya. J Mines Met Fuels, 295–297

Anderson AT (1983) Oscillatory zoning of plagioclase: Nomarski interference contrast microscopy of etched polished thin sections. Am Miner 69:660–676

Anderson AT (1984) Probable relations between plagioclase zoningand magma dynamics Fuego Volcano, Guatemala. Am Mineral 69:660–676

Anderson AT, Eklund O (1994) Cellular plagioclase intergrowths as a result of crystal-magma mixing in the Proterozoic Åland rapakivi batholith, SW Finland. Contrib Miner Petrol 117:124–136. https://doi.org/10.1007/BF00286837

Aref H, El Naschie MS (1995) Chaos applied to fluid mixing. Pergamon Press, Reprinted from: Chaos, Solutions and Fractals, 4 Exeter

Bacon CR, Druitt TH (1988) Compositional evolution of thezoned calc-alkalinemagma chamber of Mount Mazama, Crater Lake, Oregon. Contrib Miner Petrol 98:224–256. https://doi.org/10.1007/BF00402114

Baxter S, Feely M (2002) Magma mixing and mingling textures in granitoids: examples from the Galway Granite, Connemara, Ireland. Miner Petrol 76:63–74. https://doi.org/10.1007/s007100200032

Blake DH (1981) Intrusive felsic-mafic net-veined complexes in north Queensland. Bur Miner Resour J Aust Geol Geophys 6:95–99

Blasi A, Brajkovic A, De Pol BC, Foord EE, Martin RF, Zanazzi PF (1984) Structure refinement and genetic aspects of a microcline overgrowth on amazonite from Pikes Peak batholith, Colorado, U.S.A. Bull Minér 107:411–422

Blundy JD, Shimizu N (1991) Trace element evidence for plagioclase recycling in calc-alkaline magmas. Earth Planet Sci Lett 102:178–197. https://doi.org/10.1016/0012-821X(91)90007-5

Blundy JD, Sparks RSJ (1992) Petrogenesis of mafic inclusions in granitoids of the Adamello massif, Italy. J Petrol 33:1039–1104. https://doi.org/10.1093/petrology/33.5.1039

Brown WL, Parsons I (1989) Alkali feldspars: ordering rates, phase transformations and behaviour diagrams for igneous rocks. Miner Mag 53:25–42. https://doi.org/10.1180/minmag.1989.053.369.03

Castro A (2001) Plagioclase morphologies in assimilation experiments. Implications for disequilibriummelting in the generation of granodiorite rocks. Miner Petrol 71:31–49. https://doi.org/10.1007/s007100170044

Chatterjee N, Ghose NC (2011) Extensive Early Neoproterozoic high-grade metamorphism in North Chotanagpur Gneissic Complex of the Central Indian Tectonic Zone. Gondwana Res 20:362–379. https://doi.org/10.1016/j.gr.2010.12.003

Chauhan H, Tripathi A, Pandit D, Rao NVC, Ahmed T (2020) A new analytical protocol for high precision U-Th–Pb chemical dating of xenotime from the TTG gneisses of the Bundelkhand Craton, central India, using CAMECA SXFive Electron Probe Micro Analyzer. J Earth Syst Sci 129:210. https://doi.org/10.1007/s12040-020-01482-1

De Campos CP, Dingwell DB, Fehr KT (2004) Decoupled convection cells from mixing experiments with alkaline melts from Phlegrean Fields. Chem Geol 213:227–251. https://doi.org/10.1016/j.chemgeo.2004.08.045

Dhurandhar AP, Pandey UK, Raminaidu C (2019) Petrochemistry and Sr, Nd, Pb isotopic characteristics of basic Dykes of Mikir Hills, Assam. J Geol Soc India 94:559–572. https://doi.org/10.1007/s12594-019-1361-z

Domańska-Siuda J, Słaby E, Szuszkiewicz A (2019) Ambiguous isotopic and geochemical signatures resulting from limited melt interactions in a seemingly composite pluton: a case study from the Strzegom-Sobótka Massif (Sudetes, Poland). Int J Earth Sci 108(3):931–962

Dymek RF (1983) Titanium, aluminum and interlayer cation substitutionsin biotite from high-grade gneisses, west Greenland. Am Miner 68(9–10):880–899

Farner MJ, Lee CTA, Putrika KD (2014) Mafic-felsic magma mixing limited by reactive processes: a case study of biotite-rich rinds on mafic enclaves. Earth Planet Sci Lett 393:49–59. https://doi.org/10.1016/j.epsl.2014.02.040

Giannetti B, Luhr JF (1983) The white trachytic tuff of roccamonfina volcano, Italy. Contrib Miner Petrol 84:235–252. https://doi.org/10.1007/BF00371289

Gogoi B, Chauhan H (2021) Dynamics of a subvolcanic magma chamber inferred from viscousinstabilities owing to mafic-felsic magma interactions. Arab J Geosci 14:1626. https://doi.org/10.1007/s12517-021-08140-w

Gogoi B, Saikia A (2018) Synneusis: does its preservation imply magma mixing? Mineralogia 49:99–117

Gogoi B, Saikia A, Ahmad M (2018) Field evidence, mineral chemical and geochemical constraints on mafic-felsic magma interactions in a vertically zoned magma chamber from the Chotanagpur Granite Gneiss Complex of Eastern India. Chem Erde-Geochem 78:78–102. https://doi.org/10.1016/j.chemer.2017.11.003

Gogoi B, Chauhan H, Hazarika G, Baruah A, Saikia M, Hazarika PJ (2020a) Significance of viscous folding in the migmatites of Chotanagpur Granite Gneiss Complex, eastern India. Earth Environ Sci Trans R Soc Edinburgh 111:119–134

Gogoi B, Saikia A, Ahmad M (2020b) Mafic-felsic magma interactions in the Bathani volcanic-plutonic complex of Chotanagpur Granite Gneiss Complex, eastern India: implications for assembly of the Greater Indian Landmass during the Proterozoic. Episodes 43(2):785–810

Gogoi B, Chauhan H, Saikia A (2021) Understanding mafic-felsic magma interactions in a subvolcanic magma chamber using rapakivi feldspar: A case study from the Bathani volcano-sedimentary sequence, eastern India. Chem Erde-Geochem 81(2):125730

Grogan SE, Reavy RJ (2002) Disequilibrium textures in the Leinster Granite Complex, SE Ireland: evidence for acid-acid magma mixing. Miner Mag 66(6):929–939. https://doi.org/10.1180/0026461026660068

Henry DJ, Guidotti CV, Thomson JA (2005) The Ti-saturation surface for low to medium pressure metapelitic biotite: implications for geothermometry and Ti-substitution mechanisms. Am Miner 90:316–328. https://doi.org/10.2138/am.2005.1498

Hibbard MJ (1981) The magma mixing origin of mantled feldspars. Contrib Mineral Petrol 76:158–170. https://doi.org/10.1007/BF00371956

Hibbard MJ (1991) Textural anatomy of twelve magma-mixed granitoid systems. In: Didier J, Barbarin B (eds) Enclaves and granite petrology. Developments in petrology. Elsevier, Amsterdam, pp 431–444

Hildreth W (1981) Gradients in silicic magma chambers: implications for lithospheric magmatism. J Geophys Res 86:10153–10192. https://doi.org/10.1029/JB086iB11p10153

Hildreth W, Wilson CJN (2007) Compositional zoning of the Bishop Tuff. J Petrol 48:951–999. https://doi.org/10.1093/petrology/egm007

Huppert HE, Turner JS, Stephen R, Sparks J (1982) Replenished magma chambers: effects of compositional zonation and input rates. Earth Planet Sci Lett 57:345–357. https://doi.org/10.1016/0012-821X(82)90155-8

Kumar S, Rino V, Hayasaka Y, Kimura K, Raju S, Terada K, Pathak M (2017) Contribution of Columbia and Gondwana Supercontinent assembly- and growth-related magmatism in the evolution of the Meghalaya Plateau and the Mikir Hills, Northeast India: Constraints from U-Pb SHRIMP zircon geochronology and geochemistry. Lithos 277:356–375. https://doi.org/10.1016/j.lithos.2016.10.020

Leonard G, Cole J, Nairn I, Self S (2002) Basalt triggering of the c. AD 1305 Kaharoa rhyolite eruption, Tarawera Volcanic

Complex. New Zealand J Volcanol Geotherm Res 115:461–486. https://doi.org/10.1016/S0377-0273(01)00326-2
Luhr J, Carmichael ISE, Varekamp J (1984) The 1982 eruptions of El Chichon volcano, Chiapas, Mexico: mineralogy and petrology of the anhydrite-bearing pumices. J Volcanol Geotherm Res 23:69–108. https://doi.org/10.1016/0377-0273(84)90057-X
Majumdar D, Dutta P (2016) Geodynamic evolution of a Pan-African granitoid of extended Dizo Valley in Karbi Hills, NE India: Evidence from Geochemistry and Isotope Geology. J Asian Earth Sci 117:256–268
Mazumder SK (1986) The Precambrian framework of the Khasi Hills, Meghalaya. Record Geol Survey India 117:1–59
McBirney AR (1980) Mixing and unmixing in magmas. J Volcanol Geotherm Res 7:357–371. https://doi.org/10.1016/0377-0273(80)90038-4
Morimoto N, Fabries J, Ferguson AK, Ginzburg IV, Ross M, Seifert FA, Zussman J, Aoki K, Gottardi G (1988) Nomenclature of Pyroxenes. Am Miner 73:1123–1133
Murphy MD, Sparks RSJ, Barclay J, Carroll MR, Lejeune AM, Brewer TS, Macdonald R, Black S, Young S (1998) The role of magma mixing in triggering the current eruption at the Soufriere Hills Volcano, Montserrat, West Indies. Geophys Res Lett 25:3433–3436. https://doi.org/10.1029/98GL00713
Nandy DR (2001) Geodynamics of Northeastern India and the adjoining region. Acb publications, Kolkata, p 209
Ottino JM (1989) The kinematics of mixing: Stretching, chaos and transport. Cambridge University Press, Cambridge
Parsons I, Brown WL (1991) Mechanisms and kinetics of exsolution-structural control of diffusion and phase behaviour in feldspars, in: Diffusion, Atomic Ordering and Mass Transport, Advances in Physical Geochemistry, edited by: Ganguly, J., Springer-Verlag, New York, 8:304–344. https://doi.org/10.1007/978-1-4613-9019-0_10
Pearce TH, Kolisnik AM (1990) Observations of plagioclase zoning using interference imaging. Earth-Sci Rev 29:9–26. https://doi.org/10.1016/0012-8252(0)90024-P
Perugini D, Poli G (2012) The mixing of magmas in plutonic and volcanic environments: Analogies and differences. Lithos 153:261–277. https://doi.org/10.1016/j.lithos.2012.02.002
Pietranik A, Koepke J (2009) Interactions between dioritic and granodioritic magmas in mingling zones: plagioclase record of mixing, mingling and subsolidus interactions in the Gęsiniec Intrusion, NE Bohemian Massif, SW Poland. Contrib Miner Petrol 158:17–36. https://doi.org/10.1007/s00410-008-0368-z
Romero AE, McEvilly TV, Majer EL, Michelini A (1993) Velocity structure of the Long Valley caldera from the inversion of local earthquake P-travel and S-travel times. J Geophys Res 98:19869–19879. https://doi.org/10.1029/93JB01553
Singer BS, Dungan MA, Layne GD (1995) Textures and Sr, Ba, Mg, Fe, K, and Ti compositional profiles in volcanic plagioclase: clues to the dynamics of calc-alkaline magma chambers. Am Miner 80:776–798. https://doi.org/10.2138/am-1995-7-819
Singer BS, Andersen NL, Le Mével H (2014) Dynamics of a large, restless, rhyolitic magma system at Laguna del Maule, southern Andes, Chile. GSA Today 24:4–10
Słaby E, Götze J, Wörner G, Simon K, Wrzalik R, Śmigielski M (2008) K-feldspar phenocrysts in microgranular magmatic enclaves: a cathodoluminescence and geochemical study of crystal growth as a marker of magma mingling dynamics. Lithos 105:85–97
Slaby E, Götze J (2004) Feldspar crystallization under magma-mixing conditions shown by cathodoluminescence and geochemical modelling - a case study from the Karkonosze pluton (SW Poland). Mineral Mag 68:561–577
Slaby E, Martin AH (2008) Mafic and felsic magma interaction in granites: the Hercynian Karkonosze pluton (Sudetes, Bohemian Massif). J Petrol 49(2):53–391
Snyder D (1997) The mixing and mingling of magmas. Endeavour. https://doi.org/10.1016/S0160-9327(96)10032-6
Sosa-Ceballos G, Gardner JE, Siebe C, Macías JL (2012) A caldera forming eruption ~14100 14C yr BP at Popocatépetl volcano, México. Insights from eruption dynamics and magma mixing. J Volcanol Geotherm Res 212–213:27–40. https://doi.org/10.1016/j.jvolgeores.2011.11.001
Sparks RSJ, Sigurdsson H, Wilson L (1977) Magma mixing: a mechanism for triggering acid explosive eruptions. Nature 267:315–318. https://doi.org/10.1038/267315a0
Speer JA (1984) Micas in igneous rocks. Rev Mineral Geochem 13:299–356
Spera FJ, Yuen DA, Kemp DV (1984) Mass transfer rates along vertical walls in magma chambers and marginal upwelling. Nature 310:764–767. https://doi.org/10.1038/310764a0
Stamatelopoulou-Seymour K, Vlassopoulos D, Pearce TH, Rice C (1990) The record of magma chamber processes in plagioclasephenocrysts at Thera volcano, Aegean volcanic arc, Greece. Contrib Miner Petrol 104:73–84. https://doi.org/10.1007/BF00310647
Streck MJ (2008) Mineral textures and Zoning as evidence for Open System Processes. Rev Miner Geochem 69:595–622. https://doi.org/10.2138/rmg.2008.69.15
Takahashi R, Nakagawa M (2012) Formation of a compositionally reverse zoned magma chamber: petrology of the AD 1640 and 1694eruptions of Hokkaido-Komagatake Volcano, Japan. J Petrol 54:815–838. https://doi.org/10.1093/petrology/egs087
Temizel İ (2013) Petrochemical evidence of magma mingling and mixing in the Tertiary monzogabbroic stocks around the Bafra (Samsun) area in Turkey: implications of coeval mafic and felsic magma interactions. Mineral Petrol. https://doi.org/10.1007/s00710-013-0304-4
Tepley FJ III, Davidson JP, Clynne MA (1999) Magmatic interactions as recorded in plagioclase phenocrysts of Chaos Crags, Lassen volcanic center, California. J Petrol 40:787–806. https://doi.org/10.1093/petroj/40.5.787
Tizzani P, Battaglia M, Zeni G, Atzori S, Berardino P, Lanari R (2009) Uplift and magma intrusion at Long Valley Caldera from InSAR and gravity measurements. Geology 37:63–66. https://doi.org/10.1130/G25318A.1
Uchida E, Endo S, Makino M (2007) Relationship between solidification depth of granitic rocks and formation of hydrothermal ore deposits. Resour Geol 57:47–56. https://doi.org/10.1111/j.1751-3928.2006.00004.x
Vernon RH (1990) Crystallization and hybridism in microgranitoid enclave magmas: microstructural evidence. J Geophys Res 95(B11):17849–17859. https://doi.org/10.1029/JB095iB11p17849
Vernon RH, Etheridge MA, Wall VJ (1988) Shape and microstructure of microgranitoid enclaves: Indicators of magma mingling and flow. Lithos 22:1–11. https://doi.org/10.1016/0024-4937(88)90024-2
Wada H, Harayama S, Yamaguchi Y (2004) Mafic enclaves densely concentrated in the upper part of a vertically zoned felsic magma chamber: The Kurobegawa granitic pluton, Hida Mountain Range, central Japan. Geol Soc Am Bull 116:788–801
Waldron K, Parsons I, Brown WL (1993) Solution-Redeposition and the Orthoclase-Microcline Transformation: Evidence from Granulites and Relevance to 18O Exchange. Mineral Mag 57:687–595. https://doi.org/10.1180/minmag.1993.057.389.13
Wiebe RA (1994) Silicic magma chambers as traps for basaltic magma: the Cadillac Mountain intrusive complex, Mount Desert Island, Maine. J Geol 102:423–437

Wolff JA, Storey M (1984) Zoning in highly alkaline magma bodies. Geol Mag 121:563–575. https://doi.org/10.1017/S0016756800030715

Wolff JA, Warner G, Blake S (1990) Gradients in physicalparameters in zoned felsic magma bodies: implications forevolutions and eruptive withdrawal. J Volcanol Geotherm Res 43:37–55. https://doi.org/10.1016/0377-0273(90)90043-F

Wones DR, Eugster HP (1965) Stability of biotite: experiment, theory, and application. Am Mineral 50:1228–1272

Worden RH, Walker FDL, Parsons I, Brown WL (1990) Development of microporosity, diffusion channels and deuteric coarsening in perthitic alkali feldspars. Contrib Mineral Petrol 104:507–515. https://doi.org/10.1007/BF00306660

WÖrner G, Schmincke HU (1984) Mineralogical and chemical zonation of the Laacher See tephra sequence (East Eifel, W. Germany). J Petrol 25:805–835. https://doi.org/10.1093/petrology/25.4.805